A mathematical model for the release of peptide-binding drugs from affinity hydrogels

Tuoi T. N. Vo, MACSI, Department of Mathematics and Statistics, University of Limerick, Ireland. tuoi.vo@ul.ie
Martin G. Meere, School of Mathematics, Statistics and Applied Mathematics, National University of Ireland, Galway, Ireland. martin.meere@nuigalway.ie

Abstract

A mathematical model for the release of peptide-binding drugs from affinity hydrogels is analysed in detail. The model is not specific to any particular peptide/drug/gel system, and can describe drug release from a large class of affinity systems. In many cases, it is shown that the model can be reduced to a coupled pair of nonlinear partial differential equations for the total drug and peptide. Quantitative information relating the rate of drug release to the values of the model parameters is presented. Numerical solutions are displayed that illustrate the rich variety of release behaviours the system is capable of exhibiting. Theoretical release profiles generated by the model are compared with experimental release data from three different studies, and good agreement is found. The development of reliable mathematical models for affinity hydrogels will provide useful design tools for these systems.

1 Introduction

1.1 Background

Hydrogels are hydrophilic cross-linked polymer networks that have found numerous applications in the biomedical sciences [5]. Their popularity in biomedical applications is due in part to their ability to mimic some of the key features of biological tissue. In particular, they have a high water content, are soft, and permit bioactive molecules to diffuse through their open porous structure. However, unmodified hydrogels do not usually form effective reservoirs for small bioactive molecules because the composition of a hydrogel is dominated by water, and molecules can out-diffuse from the gel over a period of a few days for typical gel dimensions. Clearly, a therapy based on such a system would be of limited value if the presence of an active agent over a period of weeks or months is required, as could be the case in the context of nerve regeneration, for example.

Affinity-based drug delivery systems have been developed to overcome this deficiency [15, 29, 30]. In these systems, the hydrogel is chemically modified to enable it to bind to the active agent of interest. The binding slows the release of the molecules from the gel, and the release rate can in principle be tuned by varying the affinity of the molecules for the binding sites. Many of these systems mimic the behaviour of the extracellular matrix, which acts as a natural reservoir and protective medium for growth factors and other bioactive molecules [1, 7].

1.2 Heparin-based systems

A number of affinity drug delivery systems have been developed based on heparin. Heparin is a carbohydrate in the glycosaminoglycan family that has a high negative charge density [22]. It is used in affinity systems because it is structurally very similar to heparin sulfate and shares many of its binding properties. Heparan sulfate is a polysaccharide found in the extracellular matrix of animals [22]. It is known to bind non-covalently with a large number of growth factors, and is one of a number of proteins involved with the retention and release of growth factors from the extracellular matrix to control cellular processes. These properties make heparan sulfate an attractive material for use in synthetic affinity gels. However, heparin is preferred to heparin sulfate in the preparation of affinity gels because it shares many of the binding properties of heparan sulfate but is easier to purify.

Sakiyama-Elbert & Hubbell [18] developed a growth factor delivery system for wound healing that exploits heparin's ability to bind with growth factors. Their system consists of a three dimensional scaffold composed of a cross-linked fibrin matrix. Growth factor attaches to the matrix via a bi-domain peptide bound to heparin. The peptide contains a domain that can covalently cross-link to the fibrin matrix, and a second domain that can bind non-covalently to heparin. Heparin bound in this way can in turn bind to heparin-binding growth factors.

Hence, the interactions that bind the growth factor to the matrix in their system may be represented by (fibrin)-(peptide)-(heparin)-(growth factor). Sakiyama-Elbert & Hubbell [18] also formulated a mathematical model to describe growth factor binding and diffusion in the gel. Vo & Meere [24] analyzed this model, identified the non-dimensional parameters controlling the growth factor release rate, and compared the output of the model with experimental release profiles.

1.3 Peptide-based systems

An alternative approach is to use a peptide rather than heparin to bind drug to the matrix. Peptides are attractive choices for binding agents because they are easy to synthesize and modify, and can be readily incorporated in synthetic biomaterials. Maynard & Hubbell [14] screened a peptide library of four amino acids for heparin-like binding activity, and discovered a sulfated peptide that can bind to vascular endothelial growth factor (VEGF). Maxwell *et al.* [13] identified peptides that bound heparin with varying affinity by screening a twelve amino acid peptide library. Willerth *et al.* [31] performed a similar study to identify peptides that bind nerve growth factor (NGF). They incorporated these peptides in a fibrin-based hydrogel and demonstrated that the presence of the peptide slowed the release of NGF from the gel. They also developed a mathematical model of the reaction-diffusion type to describe the release of growth factor from their system. A variant of this model is analyzed in the current study.

Lin & Anseth [9] developed an affinity hydrogel to bind the drug streptavidin based on the compound poly(ethylene glycol) (PEG). In this system, the drug binds to a PEG network using suitably prepared peptides. They also developed PEG-based affinity gels to bind basic fibroblast growth factor (bFGF) with varying affinity, again using peptides as the binding agents. In the context of cell delivery applications, Lin *et al.* [10] and Lin *et al.* [12] developed PEG-based affinity gels to protect cells encapsulated in the gel. The purpose of these systems is not to control the delivery of a drug, but rather to retard the traffic of biological molecules *in vivo* that could harm the cells contained in the gel. This is achieved by incorporating peptides in the gel that bind to cytotoxic molecules, thereby retarding the transport of these molecules through the gel. In this manner, the gel forms a protective barrier between the encapsulated cells and the local environment *in vivo*.

Recent studies of peptide-based affinity hydrogels include those by Shepard *et al.* [19], Vulic & Shoichet [28], and Pakulska *et al.* [16]. Shepard *et al.* [19] developed a system to control the delivery of gene therapy vectors. Vulic & Shoichet [28] prepared a peptide modified hydrogel using the polysaccharides hyaluronan and methyl cellulose, and used it to modulate the release of fibroblast growth factors (FGFs). Pakulska *et al.* [16] used a peptide-based affinity gel to control the delivery of the bacterial enzyme Chrondroitinase ABC (ChABC). ChABC has received considerable attention in recent years because it has demonstrated promising results in the treatment of spinal cord injury [2].

In the current study, a mathematical model describing drug binding and diffusion in a peptide-based affinity hydrogel is analyzed in detail. Mathematical modelling is becoming an increasingly important tool in the development of drug delivery systems [20,27]. The model considered here is not specific to any particular peptide/drug/gel system, and can describe drug release from a large class of peptide-based affinity systems, including a number of those referred to above. In systems for which the diffusion time scales are long compared to the time scales associated with the binding constants, the model is reduced to a coupled pair of nonlinear partial differential equations for the concentrations of the total drug and total peptide. The parameters governing the drug release rate from the system are identified, and quantitative recommendations are made as to how the release rate may be tuned by appropriately varying these parameters. Theoretical release profiles generated by the model are compared with experimental release data available in the literature, and good agreement is found.

2 Mathematical modelling

2.1 The drug delivery system

The system discussed here encompasses a large number of affinity-based systems described in the literature. We postpone descriptions of specific affinity systems until Section 3.3, where we compare the predictions of the mathematical model with experimental data. Figure 1 shows the affinity-based drug delivery system considered in the current study. The drug molecules (circles) may be bound or unbound. The bound drug molecules are attached to a polymeric matrix via peptide molecules (rectangles) that are permanently fixed to the matrix. The unbound drug molecules are mobile and can diffuse through the gel. The system also contains free peptide, which may or

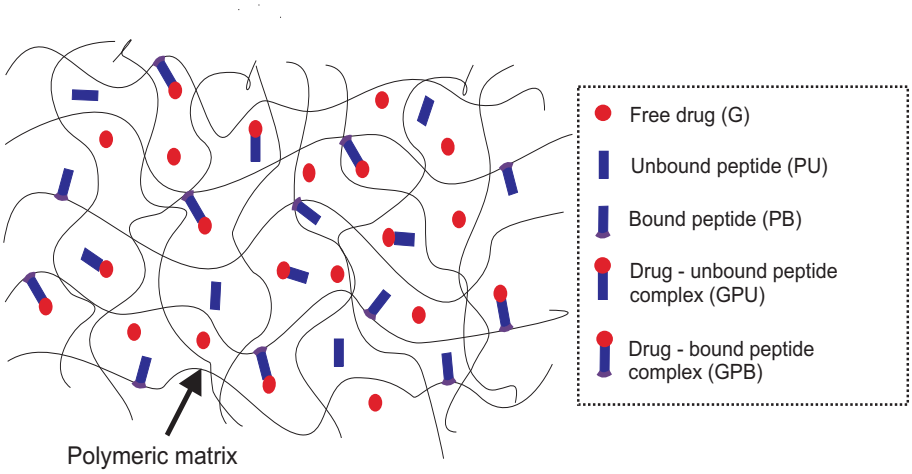

Figure 1: A schematic of the affinity hydrogel considered in this paper. The system contains five species. Bound peptide (PB) is attached to a polymeric matrix. Free drug binds with bound peptide to form drug-bound peptide complexes (GPB). Three other species are not attached to the matrix and can diffuse through the gel: these are free drug (G), unbound peptide (PU), and drug-unbound peptide complexes (GPU).

may not be bound to drug. In all, the system contains five species, and the following notation is used (Figure 1)

G is an unbound drug molecule (mobile);
PU is an unbound peptide molecule (mobile);
PB is a bound peptide molecule (immobile);
GPU is an unbound drug-peptide complex (mobile);
GPB is a bound drug-peptide complex (immobile).

Free drug may bind reversibly to either bound or unbound peptide, and these processes are represented by the chemical reactions

$$\mathrm{G}+\mathrm{PU} \underset{k_r}{\overset{k_f}{\rightleftharpoons}} \mathrm{GPU} \qquad\qquad \mathrm{G}+\mathrm{PB} \underset{k_r}{\overset{k_f}{\rightleftharpoons}} \mathrm{GPB} \tag{1}$$

where k_f, k_r are association and dissociation rate constants, respectively. In the system, bound peptide remains bound and unbound peptide remains unbound. It is noteworthy in (1) that the reaction rate constants have been assumed to be the same for the binding of drug to free peptide as for the binding of drug to bound peptide. However, it should be pointed out that this assumption may not always be valid as tethering of the peptide to the polymer network may affect the affinity of the drug for the peptide [9].

2.2 Model equations

The mathematical model described here is similar to those developed in [13] and [31]. The problems considered are one-dimensional and the spatial variable is denoted by x and the time variable by t throughout. We denote by $c_{\mathrm{G}}(x,t)$ the concentration of free drug G at location x and time t, and use a similar notation for the other four species. The partial differential equations for the five species that incorporate (1) and the assumptions made about species mobility are then

$$\begin{aligned}
\frac{\partial c_{\mathrm{G}}}{\partial t} &= D_{\mathrm{G}}\frac{\partial^2 c_{\mathrm{G}}}{\partial x^2} - k_f c_{\mathrm{G}}(c_{\mathrm{PU}}+c_{\mathrm{PB}}) + k_r(c_{\mathrm{GPU}}+c_{\mathrm{GPB}}),\\
\frac{\partial c_{\mathrm{PU}}}{\partial t} &= D_{\mathrm{PU}}\frac{\partial^2 c_{\mathrm{PU}}}{\partial x^2} - k_f c_{\mathrm{G}} c_{\mathrm{PU}} + k_r c_{\mathrm{GPU}},\\
\frac{\partial c_{\mathrm{GPU}}}{\partial t} &= D_{\mathrm{GPU}}\frac{\partial^2 c_{\mathrm{GPU}}}{\partial x^2} + k_f c_{\mathrm{G}} c_{\mathrm{PU}} - k_r c_{\mathrm{GPU}},\\
\frac{\partial c_{\mathrm{PB}}}{\partial t} &= -k_f c_{\mathrm{G}} c_{\mathrm{PB}} + k_r c_{\mathrm{GPB}},\\
\frac{\partial c_{\mathrm{GPB}}}{\partial t} &= k_f c_{\mathrm{G}} c_{\mathrm{PB}} - k_r c_{\mathrm{GPB}},
\end{aligned} \tag{2}$$

where D_{G}, D_{PU} and D_{GPU} are the constant diffusivities for the free drug, unbound peptide, and free drug-unbound peptide complex, respectively. The equations for PB and GPB do not contain diffusion terms as these species are immobile.

It is worth highlighting here one special case of the model equations (2). Suppose it is required to model a simpler system that contains no peptide and in which the drug binds directly with a suitably prepared polymeric matrix. A model for this system can be extracted from (2) by simply setting $c_{\mathrm{PU}} = c_{\mathrm{GPU}} = 0$, to obtain

$$\begin{aligned}
\frac{\partial c_{\mathrm{G}}}{\partial t} &= D_{\mathrm{G}}\frac{\partial^2 c_{\mathrm{G}}}{\partial x^2} - k_f c_{\mathrm{G}} c_{\mathrm{PB}} + k_r c_{\mathrm{GPB}},\\
\frac{\partial c_{\mathrm{PB}}}{\partial t} &= -k_f c_{\mathrm{G}} c_{\mathrm{PB}} + k_r c_{\mathrm{GPB}},\\
\frac{\partial c_{\mathrm{GPB}}}{\partial t} &= k_f c_{\mathrm{G}} c_{\mathrm{PB}} - k_r c_{\mathrm{GPB}}.
\end{aligned} \tag{3}$$

In (3), G again refers to the free drug, but PB now refers to generic unoccupied binding sites on the matrix, and GPB refers to occupied binding sites. This simpler system has previously been proposed to describe drug release from affinity hydrogels by Lin & Metters [11] and Fu *et al.* [4]. In their review of the mathematical modelling of affinity hydrogels, Vo & Meere [25] identified several affinity systems that the model can potentially describe. A comprehensive analysis of (3) in the context of drug release from affinity hydrogels will form the subject of a future study.

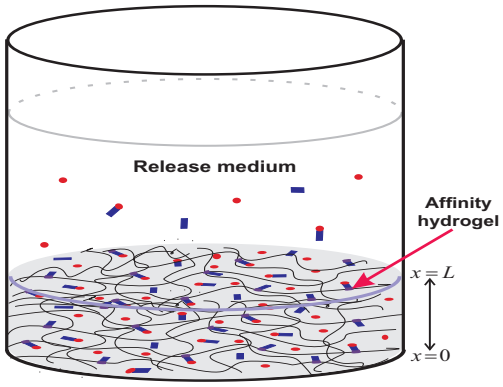

Figure 2: A typical experimental setup for the release of drug from an affinity hydrogel. The hydrogel containing the drug is in the base of an impermeable container. Dissolution medium is added to the container and drug releases into the medium from the matrix via diffusion. Specific release experiments described in the literature are considered in Section 3.3.

2.3 Boundary and initial conditions

Boundary conditions are chosen to enable comparison with as much of the published experimental data as possible. We suppose that the hydrogel occupies $0 \le x \le L$, with $x = 0$ giving the base of an impermeable container and $x = L$ denoting the interface between the gel and a fluid medium into which the drug releases; see Figure 2. At the base of the container, no-flux conditions for the mobile species are imposed

$$\frac{\partial c_{\mathrm{G}}}{\partial x}(0,t) = 0, \quad \frac{\partial c_{\mathrm{PU}}}{\partial x}(0,t) = 0, \quad \frac{\partial c_{\mathrm{GPU}}}{\partial x}(0,t) = 0 \qquad \text{for } t \ge 0. \tag{4}$$

Perfect sink conditions are imposed at the interface between the matrix and the release medium, so that

$$c_{\mathrm{G}}(L,t) = 0, \quad c_{\mathrm{PU}}(L,t) = 0, \quad c_{\mathrm{GPU}}(L,t) = 0 \qquad \text{for } t \ge 0. \tag{5}$$

Perfect sink boundary conditions are often adequate when modelling release experiments because the release medium is replaced each time a measurement is made, and the drug concentration in the medium is reset to zero with each replacement. Also, the volume of the release medium is typically more than twice that of the gel, and the drug has a larger diffusivity in water than in the gel.

Equations (2) are solved subject to the initial conditions

$$\begin{aligned}
&c_{\mathrm{G}}(x,0) = c_{\mathrm{G}}^0, \quad c_{\mathrm{PU}}(x,0) = c_{\mathrm{PU}}^0, \quad c_{\mathrm{PB}}(x,0) = c_{\mathrm{PB}}^0,\\
&c_{\mathrm{GPU}}(x,0) = c_{\mathrm{GPU}}^0, \quad c_{\mathrm{GPB}}(x,0) = c_{\mathrm{GPB}}^0 \qquad \text{for } \ 0 < x < L,
\end{aligned} \tag{6}$$

where $c_{\rm i}^0$ denotes the constant initial concentration of species i, and where i can be G, PU, PB, GPU or GPB. The question remains as to how to select appropriate values for the $c_{\rm i}^0$. This may be answered by considering the polymerization procedure for the hydrogel. In the polymerization mixture, the total concentrations for the peptide, $c_{\rm P}^{\rm T0}$, and for the growth factor, $c_{\rm G}^{\rm T0}$, are known. Clearly

$$c_{\rm G}^{\rm T0} = c_{\rm G}^0 + c_{\rm GPU}^0 + c_{\rm GPB}^0, \quad c_{\rm P}^{\rm T0} = c_{\rm PU}^0 + c_{\rm PB}^0 + c_{\rm GPU}^0 + c_{\rm GPB}^0. \tag{7}$$

The reactions in the polymerization mixture eventually reach equilibrium, so that

$$K_{bp} c_{\rm G}^0 c_{\rm PU}^0 = c_{\rm GPU}^0, \qquad K_{bp} c_{\rm G}^0 c_{\rm PB}^0 = c_{\rm GPB}^0. \tag{8}$$

Finally, if we denote by r the fraction of the total peptide that binds to the polymeric matrix during the polymerization procedure, then

$$r = \frac{c_{\rm PB}^0 + c_{\rm GPB}^0}{c_{\rm P}^{\rm T0}}. \tag{9}$$

If r is known, then (7), (8), (9) give a set of five algebraic equations for the five unknowns $c_{\rm G}^0, c_{\rm GPU}^0, c_{\rm GPB}^0, c_{\rm PU}^0, c_{\rm PB}^0$. These equations can in fact be solved explicitly, and the solution is displayed in the next subsection.

The mathematical model is now complete, and consists of equations (2) to (6).

2.4 Model reduction

We now show how the model may be reduced to a coupled pair of nonlinear partial differential equations.

2.4.1 Non-dimensionalisation

We first note that (2) may be written in the equivalent form

$$\begin{aligned}
&\frac{\partial}{\partial t}(c_{\rm G} + c_{\rm GPU} + c_{\rm GPB}) = D_{\rm G}\frac{\partial^2 c_{\rm G}}{\partial x^2} + D_{\rm GPU}\frac{\partial^2 c_{\rm GPU}}{\partial x^2},\\
&\frac{\partial}{\partial t}(c_{\rm PU} + c_{\rm PB} + c_{\rm GPU} + c_{\rm GPB}) = D_{\rm PU}\frac{\partial^2 c_{\rm PU}}{\partial x^2} + D_{\rm GPU}\frac{\partial^2 c_{\rm GPU}}{\partial x^2},\\
&\frac{\partial c_{\rm GPU}}{\partial t} = D_{\rm GPU}\frac{\partial^2 c_{\rm GPU}}{\partial x^2} + k_f c_{\rm G} c_{\rm PU} - k_r c_{\rm GPU},\\
&\frac{\partial c_{\rm GPB}}{\partial t} = k_f c_{\rm G} c_{\rm PB} - k_r c_{\rm GPB},\\
&c_{\rm PB} + c_{\rm GPB} = c_{\rm PB}^0 + c_{\rm GPB}^0,
\end{aligned} \tag{10}$$

where, for example, equation $(10)_1$ is obtained by forming $(2)_1$+$(2)_3$+ $(2)_5$. We denote the total concentrations of drug and peptide in the hydrogel at location x and time t by $c_{\rm G}^{\rm T}(x,t)$ and $c_{\rm P}^{\rm T}(x,t)$, respectively, so that

$$\begin{aligned}
c_{\rm G}^{\rm T}(x,t) &= c_{\rm G}(x,t) + c_{\rm GPU}(x,t) + c_{\rm GPB}(x,t),\\
c_{\rm P}^{\rm T}(x,t) &= c_{\rm PU}(x,t) + c_{\rm PB}(x,t) + c_{\rm GPU}(x,t) + c_{\rm GPB}(x,t).
\end{aligned} \tag{11}$$

Equations $(10)_1$ and $(10)_2$ give the evolution equations for the total drug and peptide, and may be written in conservation form as

$$\frac{\partial c_{\rm G}^{\rm T}}{\partial t} + \frac{\partial j_{\rm G}^{\rm T}}{\partial x} = 0, \qquad \frac{\partial c_{\rm P}^{\rm T}}{\partial t} + \frac{\partial j_{\rm P}^{\rm T}}{\partial x} = 0, \tag{12}$$

where

$$j_{\rm G}^{\rm T} = -D_{\rm G}\frac{\partial c_{\rm G}}{\partial x} - D_{\rm GPU}\frac{\partial c_{\rm GPU}}{\partial x}, \qquad j_{\rm P}^{\rm T} = -D_{\rm PU}\frac{\partial c_{\rm PU}}{\partial x} - D_{\rm GPU}\frac{\partial c_{\rm GPU}}{\partial x}, \tag{13}$$

give the total flux of drug and peptide, respectively.

We introduce non-dimensional variables as follows

$$\begin{aligned}
&\bar{x} = \frac{x}{L}, \quad \bar{t} = \frac{t}{(L^2/D_{\rm GPU})}, \quad \bar{c}_{\rm G} = \frac{c_{\rm G}}{c_{\rm G}^{\rm T0}}, \quad \bar{c}_{\rm GPU} = \frac{c_{\rm GPU}}{c_{\rm G}^{\rm T0}}, \quad \bar{c}_{\rm GPB} = \frac{c_{\rm GPB}}{c_{\rm G}^{\rm T0}}, \quad \bar{c}_{\rm PU} = \frac{c_{\rm PU}}{c_{\rm P}^{\rm T0}},\\
&\bar{c}_{\rm PB} = \frac{c_{\rm PB}}{c_{\rm P}^{\rm T0}}, \quad \bar{c}_{\rm G}^{\rm T} = \frac{c_{\rm G}^{\rm T}}{c_{\rm G}^{\rm T0}}, \quad \bar{c}_{\rm P}^{\rm T} = \frac{c_{\rm P}^{\rm T}}{c_{\rm P}^{\rm T0}}, \quad \bar{j}_{\rm G}^{\rm T} = \frac{j_{\rm G}^{\rm T}}{(D_{\rm GPU} c_{\rm G}^{\rm T0}/L)}, \quad \bar{j}_{\rm P}^{\rm T} = \frac{j_{\rm P}^{\rm T}}{(D_{\rm GPU} c_{\rm P}^{\rm T0}/L)},
\end{aligned}$$

to obtain the following non-dimensional form for the governing initial boundary value problem (dropping the over-bars for convenience)

$$\begin{aligned}
&\frac{\partial}{\partial t}(c_{\mathrm{G}}+c_{\mathrm{GPU}}+c_{\mathrm{GPB}})=D^{*}_{\mathrm{G}}\frac{\partial^2 c_{\mathrm{G}}}{\partial x^2}+\frac{\partial^2 c_{\mathrm{GPU}}}{\partial x^2},\\
&\frac{\partial}{\partial t}\left(c_{\mathrm{PU}}+c_{\mathrm{PB}}+\frac{1}{\eta_{\mathrm{P/G}}}(c_{\mathrm{GPU}}+c_{\mathrm{GPB}})\right)=D^{*}_{\mathrm{PU}}\frac{\partial^2 c_{\mathrm{PU}}}{\partial x^2}+\frac{1}{\eta_{\mathrm{P/G}}}\frac{\partial^2 c_{\mathrm{GPU}}}{\partial x^2},\\
&\delta_{\mathrm{G}}\frac{\partial c_{\mathrm{GPU}}}{\partial t}=\delta_{\mathrm{G}}\frac{\partial^2 c_{\mathrm{GPU}}}{\partial x^2}+K_{b\mathrm{P}}c_{\mathrm{G}}c_{\mathrm{PU}}-c_{\mathrm{GPU}},\\
&\delta_{\mathrm{G}}\frac{\partial c_{\mathrm{GPB}}}{\partial t}=K_{b\mathrm{P}}c_{\mathrm{G}}c_{\mathrm{PB}}-c_{\mathrm{GPB}},\\
&\eta_{\mathrm{P/G}}c_{\mathrm{PB}}+c_{\mathrm{GPB}}=r\eta_{\mathrm{P/G}},
\end{aligned}\tag{14}$$

where

$$\begin{aligned}
&D^{*}_{\mathrm{G}}=\frac{D_{\mathrm{G}}}{D_{\mathrm{GPU}}},\quad D^{*}_{\mathrm{PU}}=\frac{D_{\mathrm{PU}}}{D_{\mathrm{GPU}}},\quad \eta_{\mathrm{P/G}}=\frac{c_{\mathrm{P}}^{\mathrm{T0}}}{c_{\mathrm{G}}^{\mathrm{T0}}},\\
&\delta_{\mathrm{G}}=\frac{D_{\mathrm{GPU}}}{k_r L^2},\quad K_{b\mathrm{P}}=\frac{k_f c_{\mathrm{P}}^{\mathrm{T0}}}{k_r},
\end{aligned}\tag{15}$$

are the governing non-dimensional parameters.

Estimates for the parameters (15) for some real systems are given in the next subsection. The parameters D^{*}_{G} and D^{*}_{PU} depend on the diffusive properties of the drug and the peptide in the gel, and are fixed for a given drug/petptide/gel system. The fraction $\eta_{\mathrm{P/G}}$ measures the initial ratio of peptide to drug in the system, and is a quantity that may be readily varied in experiments. The parameter r gives the fraction of the total peptide that has bound to the polymeric matrix, and δ_{G} measures the diffusion time scale in the gel to the dissociation time scale. The most important parameter in determining the drug release rate is usually the binding parameter $K_{b\mathrm{P}}$. This parameter may be written as

$$K_{b\mathrm{P}}=\frac{c_{\mathrm{P}}^{\mathrm{T0}}}{K^{\mathrm{D}}_{\mathrm{G\text{-}P}}}\tag{16}$$

where $K^{\mathrm{D}}_{\mathrm{G\text{-}P}}=k_r/k_f$ is the dissociation constant. $K_{b\mathrm{P}}\gg 1$ implies that the drug is strongly retained by the matrix, and $K_{b\mathrm{P}}\ll 1$ corresponds to weak drug retention. It is noteworthy that $K_{b\mathrm{P}}$ depends on both the dissociation constant and the concentration of available binding sites. In this paper, when we refer to a drug being *strongly retained* by the hydrogel, we mean that $K_{b\mathrm{P}}\gg 1$.

The non-dimensional forms for the total growth factor and peptide and their fluxes are given by

$$\begin{aligned}
&c^{\mathrm{T}}_{\mathrm{G}}(x,t)=c_{\mathrm{G}}(x,t)+c_{\mathrm{GPU}}(x,t)+c_{\mathrm{GPB}}(x,t),\\
&c^{\mathrm{T}}_{\mathrm{P}}(x,t)=c_{\mathrm{PU}}(x,t)+c_{\mathrm{PB}}(x,t)+\frac{1}{\eta_{\mathrm{P/G}}}(c_{\mathrm{GPU}}(x,t)+c_{\mathrm{GPB}}(x,t)),\\
&j^{\mathrm{T}}_{\mathrm{G}}=-D^{*}_{\mathrm{G}}\frac{\partial c_{\mathrm{G}}}{\partial x}-\frac{\partial c_{\mathrm{GPU}}}{\partial x},\qquad j^{\mathrm{T}}_{\mathrm{P}}=-D^{*}_{\mathrm{PU}}\frac{\partial c_{\mathrm{PU}}}{\partial x}-\frac{1}{\eta_{\mathrm{P/G}}}\frac{\partial c_{\mathrm{GPU}}}{\partial x}.
\end{aligned}\tag{17}$$

We denote by $M(t)$ the total amount of drug that has released from the hydrogel by time t. The fraction of the total drug load that has released by time t is given in non-dimensional variables by

$$\frac{M(t)}{M(\infty)}=1-\int_0^1 c^{\mathrm{T}}_{\mathrm{G}}(x,t)dx.\tag{18}$$

In this study, plots of $M(t)/M(\infty)$ versus t are referred to as release profiles.

2.4.2 Parameter values

In Table 1, we display numerical values for the parameters appearing in the mathematical model. These values have been taken from the published literature, and the relevant references can be found in the table. Other sources of information concerning parameter values can be found in these references. It is worth making one remark concerning time scales here. Taking $D=1.0\times 10^{-4}$ cm^{2}min^{-1} as a representative diffusivity for a species in the gel and the gel thickness to be $L=0.2$ cm, we calculate a typical diffusion time scale to be $L^2/D\approx 7$ hours. However, the time scales associated with the binding reactions are frequently much shorter. For example, taking $k_r=1$ min^{-1} and $k_f\approx 4\times 10^5$ M^{-1} min^{-1} for the binding constants and $c_{\mathrm{P}}^{\mathrm{T0}}=2.5\times 10^{-4}$ M for the initial peptide concentration gives the binding time scales $1/k_r=1$ min and $1/(k_f c_{\mathrm{P}}^{\mathrm{T0}})\approx 1$ s.

Table 1: Some values for the parameters arising in the mathematical model. These values are taken from the published literature.

Symbol	Value	Description	Reference
D_{G}	9.7×10^{-5} cm^2/min	Diffusivity of NGF	[33]
	6.0×10^{-5} cm^2/min	Diffusivity of bFGF	[18]
	1.0×10^{-4} cm^2/min	Diffusivity of NGF	[31]
	9.1×10^{-5} cm^2/min	Diffusivity of heparin	[33]
	3.1×10^{-5} cm^2/min	Diffusivity of heparin	[18]
	5.4×10^{-5} cm^2/min	Diffusivity of heparin	[13]
	1.0×10^{-5} cm^2/min	Diffusivity of bFGF-heparin complex	[18]
	7.5×10^{-5} cm^2/min	Diffusivity of NGF-heparin complex	[33]
D_{PU}	1.8×10^{-4} cm^2/min	Diffusivity of peptide	[31]
	1.9×10^{-4} cm^2/min	Diffusivity of peptide	[33]
	9.0×10^{-5} cm^2/min	Diffusivity of peptide	[13]
D_{GPU}	9.6×10^{-5} cm^2/min	Diffusivity of NGF-peptide complex	[31]
	5.0×10^{-5} cm^2/min	Diffusivity of heparin-peptide complex	[13]
	8.6×10^{-5} cm^2/min	Diffusivity of heparin-peptide complex	[33]
k_f	9.0×10^{8} M^{-1}min^{-1}	Association rate for peptide and heparin	[13]
	2.9×10^{3} M^{-1} min^{-1}	Association rate for peptide and VEGF	[14]
	2.8×10^{5} M^{-1} min^{-1}	Association rate for peptide and NGF (pH 6.0)	[31]
	4.6×10^{5} M^{-1} min^{-1}	Association rate for peptide and NGF (pH 4.5)	[31]
	3.3×10^{5} M^{-1} min^{-1}	Association rate for peptide and NGF (pH 2.8)	[31]
k_r	78 min^{-1}	Dissociation rate for peptide and heparin	[18]
	60 min^{-1}	Dissociation rate for peptide and NGF	[31]
	8.4×10^{-3} min^{-1}	Dissociation rate for peptide and VEGF	[14]
c_{P}^0	2.5×10^{-4}M	Initial concentration of peptide	[31]
	4.55×10^{-4}M	Initial concentration of peptide	[16]
L	0.2 cm	Thickness of affinity hydrogel	[13, 31]

2.4.3 Reduction to a pair of coupled partial differential equations

The previous subsection and Table 1 suggest that

$$\frac{L^2}{D_{\text{GPU}}} \gg \frac{1}{k_r}, \quad \frac{1}{k_f c_{\text{P}}^{\text{T}0}},$$

for many systems. In terms of the dimensionless parameters (15), these conditions correspond to $\delta_{\text{G}} \ll \min(K_{b\text{P}}, 1)$. We restrict our attention to such cases in the current analysis, and set $\delta_{\text{G}} = 0$ in $(14)_3$ and $(14)_4$ to obtain

$$K_{b\text{P}} c_{\text{G}} c_{\text{PU}} = c_{\text{GPU}}, \quad K_{b\text{P}} c_{\text{G}} c_{\text{PB}} = c_{\text{GPB}}. \tag{19}$$

These expressions correspond to the equilibrium forms for the binding of drug to unbound and bound peptide, respectively.

We can now write the concentrations of the five species c_{G}, c_{PU}, c_{PB}, c_{GPU}, and c_{GPB} in terms of the total concentration of drug, $c_{\text{G}}^{\text{T}}(x,t)$, and peptide, $c_{\text{P}}^{\text{T}}(x,t)$, by solving the five algebraic expressions $(14)_5$, $(17)_1$, $(17)_2$ and (19). This yields

$$\begin{aligned}
c_{\text{G}}(c_{\text{G}}^{\text{T}}, c_{\text{P}}^{\text{T}}) &= \frac{K_{b\text{P}}\,(c_{\text{G}}^{\text{T}} - \eta_{\text{P/G}} c_{\text{P}}^{\text{T}}) - \eta_{\text{P/G}} + \sqrt{\left[K_{b\text{P}}\,(c_{\text{G}}^{\text{T}} - \eta_{\text{P/G}} c_{\text{P}}^{\text{T}}) - \eta_{\text{P/G}}\right]^2 + 4K_{b\text{P}}\eta_{\text{P/G}} c_{\text{G}}^{\text{T}}}}{2K_{b\text{P}}}, \\
c_{\text{PU}}(c_{\text{G}}^{\text{T}}, c_{\text{P}}^{\text{T}}) &= \frac{\eta_{\text{P/G}}(c_{\text{P}}^{\text{T}} - r)}{\eta_{\text{P/G}} + K_{b\text{P}} c_{\text{G}}(c_{\text{G}}^{\text{T}}, c_{\text{P}}^{\text{T}})}, \\
c_{\text{GPU}}(c_{\text{G}}^{\text{T}}, c_{\text{P}}^{\text{T}}) &= \eta_{\text{P/G}}\,(c_{\text{P}}^{\text{T}} - r - c_{\text{PU}}(c_{\text{G}}^{\text{T}}, c_{\text{P}}^{\text{T}}))\,, \\
c_{\text{GPB}}(c_{\text{G}}^{\text{T}}, c_{\text{P}}^{\text{T}}) &= c_{\text{G}}^{\text{T}} - c_{\text{G}}(c_{\text{G}}^{\text{T}}, c_{\text{P}}^{\text{T}}) - c_{\text{GPU}}(c_{\text{G}}^{\text{T}}, c_{\text{P}}^{\text{T}}), \\
c_{\text{PB}}(c_{\text{G}}^{\text{T}}, c_{\text{P}}^{\text{T}}) &= r - \frac{c_{\text{GPB}}(c_{\text{G}}^{\text{T}}, c_{\text{P}}^{\text{T}})}{\eta_{\text{P/G}}}.
\end{aligned} \tag{20}$$

It is now clear that it is sufficient to solve for c_{G}^{T} and c_{P}^{T} in our problem as the concentrations for c_{G}, c_{PU}, c_{PB}, c_{GPU}, and c_{GPB} then follow immediately from (20).

The expressions (20) imply that we can replace (14) by the following problem containing just two coupled partial differential equations

$$\begin{aligned}
&\frac{\partial c_{\text{G}}^{\text{T}}}{\partial t} + \frac{\partial}{\partial x}\; j_{\text{G}}^{\text{T}}(c_{\text{G}}^{\text{T}}, c_{\text{P}}^{\text{T}}, c_{\text{G}x}^{\text{T}}, c_{\text{P}x}^{\text{T}}) = 0, \\
&\frac{\partial c_{\text{P}}^{\text{T}}}{\partial t} + \frac{\partial}{\partial x}\; j_{\text{P}}^{\text{T}}(c_{\text{G}}^{\text{T}}, c_{\text{P}}^{\text{T}}, c_{\text{G}x}^{\text{T}}, c_{\text{P}x}^{\text{T}}) = 0, \\
&\frac{\partial c_{\text{G}}^{\text{T}}}{\partial x}(0,t) = 0, \;\; \frac{\partial c_{\text{P}}^{\text{T}}}{\partial x}(0,t) = 0 \;\; \text{for } t \geq 0, \\
&c_{\text{G}}^{\text{T}}(1,t) = 0, \;\; c_{\text{P}}^{\text{T}}(1,t) = r \;\; \text{for } t \geq 0, \\
&c_{\text{G}}^{\text{T}}(x,0) = 1, \;\; c_{\text{P}}^{\text{T}}(x,0) = 1 \;\; \text{for } 0 < x < 1,
\end{aligned} \tag{21}$$

where

$$j_{\text{G}}^{\text{T}}(c_{\text{G}}^{\text{T}}, c_{\text{P}}^{\text{T}}, c_{\text{G}x}^{\text{T}}, c_{\text{P}x}^{\text{T}}) = -D_{\text{G}}^{*} \frac{\partial}{\partial x}\; c_{\text{G}}(c_{\text{G}}^{\text{T}}, c_{\text{P}}^{\text{T}}) - \frac{\partial}{\partial x}\; c_{\text{GPU}}(c_{\text{G}}^{\text{T}}, c_{\text{P}}^{\text{T}}),$$

$$j_{\text{P}}^{\text{T}}(c_{\text{G}}^{\text{T}}, c_{\text{P}}^{\text{T}}, c_{\text{G}x}^{\text{T}}, c_{\text{P}x}^{\text{T}}) = -D_{\text{PU}}^{*} \frac{\partial}{\partial x}\; c_{\text{PU}}(c_{\text{G}}^{\text{T}}, c_{\text{P}}^{\text{T}}) - \frac{1}{\eta_{\text{P/G}}} \frac{\partial}{\partial x}\; c_{\text{GPU}}(c_{\text{G}}^{\text{T}}, c_{\text{P}}^{\text{T}}),$$

and the expressions for $c_{\text{G}}(c_{\text{G}}^{\text{T}}, c_{\text{P}}^{\text{T}})$, $c_{\text{GPU}}(c_{\text{G}}^{\text{T}}, c_{\text{P}}^{\text{T}})$ and $c_{\text{PU}}(c_{\text{G}}^{\text{T}}, c_{\text{P}}^{\text{T}})$ are given in (20). We note that (21) is in a standard form that can be readily given to a mathematical package such as MAPLE or MATLAB to solve.

Equations $(21)_1$ and $(21)_2$ may also be written in the form

$$\frac{\partial \mathbf{c}^{\text{T}}}{\partial t} = \frac{\partial}{\partial x}\left(\mathbf{D}(\mathbf{c}^{\text{T}}) \frac{\partial \mathbf{c}^{\text{T}}}{\partial x}\right) \quad \text{where} \quad \mathbf{c}^{\text{T}} = \begin{pmatrix} c_{\text{G}}^{\text{T}} \\ c_{\text{P}}^{\text{T}} \end{pmatrix},$$

and where $\mathbf{D}(\mathbf{c}^{\text{T}})$ is a diffusion matrix for the system given by

$$\mathbf{D}(\mathbf{c}^{\text{T}}) = \begin{pmatrix} D_{\text{GG}}^{\text{T}}(\mathbf{c}^{\text{T}}) & D_{\text{GP}}^{\text{T}}(\mathbf{c}^{\text{T}}) \\ D_{\text{PG}}^{\text{T}}(\mathbf{c}^{\text{T}}) & D_{\text{PP}}^{\text{T}}(\mathbf{c}^{\text{T}}) \end{pmatrix},$$

with

$$D^{\mathrm{T}}_{\mathrm{GG}}(\mathbf{c}^{\mathrm{T}}) = D^{*}_{\mathrm{G}}\frac{\partial c_{\mathrm{G}}}{\partial c^{\mathrm{T}}_{\mathrm{G}}}(\mathbf{c}^{\mathrm{T}}) + \frac{\partial c_{\mathrm{GPU}}}{\partial c^{\mathrm{T}}_{\mathrm{G}}}(\mathbf{c}^{\mathrm{T}}),\;\; D^{\mathrm{T}}_{\mathrm{GP}}(\mathbf{c}^{\mathrm{T}}) = D^{*}_{\mathrm{G}}\frac{\partial c_{\mathrm{G}}}{\partial c^{\mathrm{T}}_{\mathrm{P}}}(\mathbf{c}^{\mathrm{T}}) + \frac{\partial c_{\mathrm{GPU}}}{\partial c^{\mathrm{T}}_{\mathrm{P}}}(\mathbf{c}^{\mathrm{T}}),$$
$$D^{\mathrm{T}}_{\mathrm{PG}}(\mathbf{c}^{\mathrm{T}}) = D^{*}_{\mathrm{PU}}\frac{\partial c_{\mathrm{PU}}}{\partial c^{\mathrm{T}}_{\mathrm{G}}}(\mathbf{c}^{\mathrm{T}}) + \frac{1}{\eta_{\mathrm{P/G}}}\frac{\partial c_{\mathrm{GPU}}}{\partial c^{\mathrm{T}}_{\mathrm{G}}}(\mathbf{c}^{\mathrm{T}}),\; D^{\mathrm{T}}_{\mathrm{PP}}(\mathbf{c}^{\mathrm{T}}) = D^{*}_{\mathrm{PU}}\frac{\partial c_{\mathrm{PU}}}{\partial c^{\mathrm{T}}_{\mathrm{P}}}(\mathbf{c}^{\mathrm{T}}) + \frac{1}{\eta_{\mathrm{P/G}}}\frac{\partial c_{\mathrm{GPU}}}{\partial c^{\mathrm{T}}_{\mathrm{P}}}(\mathbf{c}^{\mathrm{T}}). \tag{22}$$

In this notation, the fluxes may be written as

$$\mathbf{j}^{\mathrm{T}} = -\mathbf{D}(\mathbf{c}^{\mathrm{T}})\frac{\partial \mathbf{c}^{\mathrm{T}}}{\partial x} \qquad \text{where} \qquad \mathbf{j}^{\mathrm{T}} = \begin{pmatrix} j^{\mathrm{T}}_{\mathrm{G}} \\ j^{\mathrm{T}}_{\mathrm{P}} \end{pmatrix}.$$

We remark that drug diffusion against the drug concentration gradient is possible in this system for appropriate choices of initial and boundary conditions since, for example

$$\frac{\partial c^{\mathrm{T}}_{\mathrm{G}}}{\partial x} < 0 \quad \text{and} \quad j^{\mathrm{T}}_{\mathrm{G}} < 0 \quad \text{provided} \quad -D^{\mathrm{T}}_{\mathrm{GG}}\frac{\partial c^{\mathrm{T}}_{\mathrm{G}}}{\partial x} < D^{\mathrm{T}}_{\mathrm{GP}}\frac{\partial c^{\mathrm{T}}_{\mathrm{P}}}{\partial x}$$

3 Results and discussion

3.1 No free peptide

We begin with the case where all of the peptide is bound to the matrix, so that there is no free peptide in the gel. This case is important because free peptide typically exits a system over a relatively short diffusion time scale once the gel has been placed in a fluid environment. Free peptide cannot be replenished by the matrix because bound peptide remains bound in the systems considered here.

We revert to dimensional quantities in this section for clarity, although we continue to use the dimensionless binding parameter $K_{b\mathrm{P}}$ for convenience. The case of no free peptide corresponds to $c^{0}_{\mathrm{PU}} = c^{0}_{\mathrm{GPU}} = 0$, so that $c^{\mathrm{T}0}_{\mathrm{P}} = c^{0}_{\mathrm{PB}} + c^{0}_{\mathrm{GPB}}$ and $r = 1$. For $r = 1$, it follows from (20) and (21) that

$$c^{\mathrm{T}}_{\mathrm{P}} = c^{\mathrm{T}0}_{\mathrm{P}}, \;\; c_{\mathrm{PU}} = 0, \;\; c_{\mathrm{GPU}} = 0,$$

and

$$\begin{aligned} &\frac{\partial c^{\mathrm{T}}_{\mathrm{G}}}{\partial t} = \frac{\partial}{\partial x}\left(D^{\mathrm{T}}_{\mathrm{GG}}(c^{\mathrm{T}}_{\mathrm{G}})\frac{\partial c^{\mathrm{T}}_{\mathrm{G}}}{\partial x}\right), \\ &\frac{\partial c^{\mathrm{T}}_{\mathrm{G}}}{\partial x}(0,t) = 0 \;\; \text{for } t \geq 0, \\ &c^{\mathrm{T}}_{\mathrm{G}}(L,t) = 0 \;\; \text{for } t \geq 0, \\ &c^{\mathrm{T}}_{\mathrm{G}}(x,0) = c^{\mathrm{T}0}_{\mathrm{G}} \;\; \text{for } 0 < x < L, \end{aligned} \tag{23}$$

where

$$D^{\mathrm{T}}_{\mathrm{GG}}(c^{\mathrm{T}}_{\mathrm{G}}) = \frac{D_{\mathrm{G}}}{2}\left(1 + \frac{K_{b\mathrm{P}}\,(c^{\mathrm{T}}_{\mathrm{G}}/c^{\mathrm{T}0}_{\mathrm{P}} - 1) + 1}{\sqrt{\left[K_{b\mathrm{P}}\,(c^{\mathrm{T}}_{\mathrm{G}}/c^{\mathrm{T}0}_{\mathrm{P}} - 1) - 1\right]^2 + 4K_{b\mathrm{P}}c^{\mathrm{T}}_{\mathrm{G}}/c^{\mathrm{T}0}_{\mathrm{P}}}}\right). \tag{24}$$

Hence, for the case of no free peptide, the transport of the total drug is encapsulated in a concentration dependent effective diffusivity. An elementary calculation shows that

$$D^{\mathrm{T}}_{\mathrm{GG}}(c^{\mathrm{T}}_{\mathrm{G}}) \leq D_{\mathrm{G}}$$

so that the effective diffusivity is less than the diffusivity for the free drug. This is as expected since the total drug contains a bound fraction, whereas all of the free drug is mobile. We also have $D^{\mathrm{T}}_{\mathrm{GG}}(c^{\mathrm{T}}_{\mathrm{G}}) \to D_{\mathrm{G}}/(1+K_{b\mathrm{P}})$ as $c^{\mathrm{T}}_{\mathrm{G}}/c^{\mathrm{T}0}_{\mathrm{P}} \to 0$, $D^{\mathrm{T}}_{\mathrm{GG}}(c^{\mathrm{T}}_{\mathrm{G}}) \to D_{\mathrm{G}}$ as $c^{\mathrm{T}}_{\mathrm{G}}/c^{\mathrm{T}0}_{\mathrm{P}} \to \infty$, and $D^{\mathrm{T}}_{\mathrm{GG}}(c^{\mathrm{T}}_{\mathrm{G}})$ is an increasing function of $c^{\mathrm{T}}_{\mathrm{G}}$. In Figure 3, we plot $D^{\mathrm{T}}_{\mathrm{GG}}(c^{\mathrm{T}}_{\mathrm{G}})/D_{\mathrm{G}}$ as a function of $c^{\mathrm{T}}_{\mathrm{G}}/c^{\mathrm{T}0}_{\mathrm{P}}$ for various values of $K_{b\mathrm{P}}$.

Concentration-dependent diffusion coefficients arise in numerous contexts in applications, and some discussion of their mathematics is given in Chapter 7 of Crank [3]. One particularly interesting diffusion coefficient is that formulated by Hu & Schmidt [6], and subsequently analyzed by King & Please [8] and Please & King [17]. This coefficient describes impurity diffusion through a silicon crystal, and it shares some notable similarities with (24).

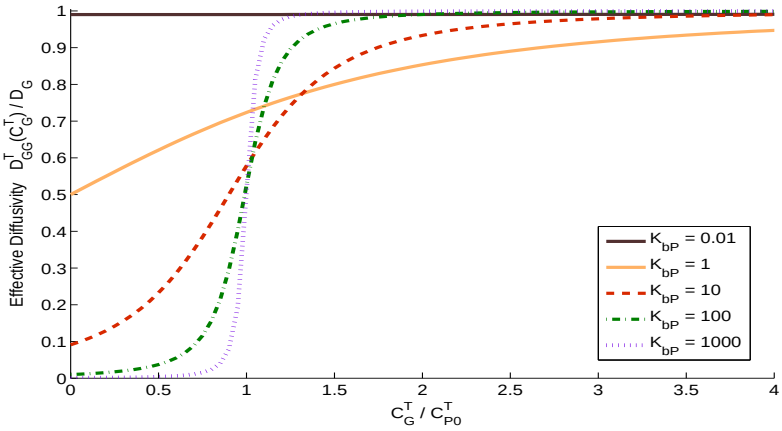

Figure 3: Plots of the effective diffusivity $D^{\mathrm{T}}_{\mathrm{GG}}(c^{\mathrm{T}}_{\mathrm{G}})/D_{\mathrm{G}}$ as a function of $c^{\mathrm{T}}_{\mathrm{G}}/c^{\mathrm{T0}}_{\mathrm{P}}$ for various values of $K_{b\mathrm{P}}$. The step-like behaviour discussed in the main text is evident in those curves that have $K_{b\mathrm{P}} \gg 1$.

3.1.1 No free peptide and strongly retained drug

We now consider the subcase where there is no free peptide in the system and the drug is strongly retained by the gel. The results obtained here are of interest when slow drug release over a period of weeks or months is desired, or when it is required to maintain the drug in the gel until it is released by invading cells [32].

Strongly retained drug corresponds to the case $K_{b\mathrm{P}} \gg 1$, or, $c^{\mathrm{T0}}_{\mathrm{P}} \gg K^{\mathrm{D}}_{\mathrm{G\text{-}P}}$. An asymptotic analysis of the initial boundary value problem (23) in the limit $K_{b\mathrm{P}} \to \infty$ is given in Section 4.3 of [26], and is reviewed in the appendix of this paper. The results of this analysis are very briefly summarized here. For related studies, see [21] and [23]. Taking the limit $K_{b\mathrm{P}} \to \infty$ in (24) with $c^{\mathrm{T}}_{\mathrm{G}}/c^{\mathrm{T0}}_{\mathrm{P}} = O(1)$ gives

$$D^{\mathrm{T}}_{\mathrm{GG}}(c^{\mathrm{T}}_{\mathrm{G}}) \sim \begin{cases} D_{\mathrm{G}} & \text{for } c^{\mathrm{T}}_{\mathrm{G}} > c^{\mathrm{T0}}_{\mathrm{P}}, \\ \frac{1}{2} D_{\mathrm{G}} \left(1 + \frac{\alpha}{\sqrt{\alpha^2+4}}\right) & \text{for } \alpha = O(1) \ \text{ where } \ c^{\mathrm{T}}_{\mathrm{G}} = c^{\mathrm{T0}}_{\mathrm{P}} \left(1 + \frac{1}{\sqrt{K_{b\mathrm{P}}}}\alpha\right), \\ K^{-1}_{b\mathrm{P}} \left\{ D_{\mathrm{G}} / (c^{\mathrm{T}}_{\mathrm{G}}/c^{\mathrm{T0}}_{\mathrm{P}} - 1)^2 \right\} \ll D_{\mathrm{G}} & \text{for } c^{\mathrm{T}}_{\mathrm{G}} < c^{\mathrm{T0}}_{\mathrm{P}}, \end{cases} \tag{25}$$

and $D^{\mathrm{T}}_{\mathrm{GG}}(c^{\mathrm{T}}_{\mathrm{G}}) = D_{\mathrm{G}} H(c^{\mathrm{T}}_{\mathrm{G}} - c^{\mathrm{T0}}_{\mathrm{P}})$ for $K_{b\mathrm{P}} = \infty$ where H is a Heaviside step function. The step-like behaviour predicted by (25) is evident in Figure 3 for those curves that have $K_{b\mathrm{P}} \gg 1$, and is easily interpreted. At locations where $c^{\mathrm{T}}_{\mathrm{G}} > c^{\mathrm{T0}}_{\mathrm{P}}$, the drug concentration exceeds the concentration of available binding sites, and there is a fraction of unbound drug that is free to diffuse. This determines the fast effective diffusion rate $D^{\mathrm{T}}_{\mathrm{GG}}(c^{\mathrm{T}}_{\mathrm{G}}) \sim D_{\mathrm{G}}$ for $c^{\mathrm{T}}_{\mathrm{G}} > c^{\mathrm{T0}}_{\mathrm{P}}$. However, at locations where $c^{\mathrm{T}}_{\mathrm{G}} < c^{\mathrm{T0}}_{\mathrm{P}}$, there are sufficient binding sites to accommodate all of the drug to leading order, and the effective diffusion rate is slow, with $D^{\mathrm{T}}_{\mathrm{GG}}(c^{\mathrm{T}}_{\mathrm{G}}) = O(D_{\mathrm{G}}/K_{b\mathrm{P}}) \ll D_{\mathrm{G}}$ for $c^{\mathrm{T}}_{\mathrm{G}} < c^{\mathrm{T0}}_{\mathrm{P}}$. The intermediate expression in (25) gives the transition between the fast and the slow rates over a narrow region near $c^{\mathrm{T}}_{\mathrm{G}} = c^{\mathrm{T0}}_{\mathrm{P}}$. These behaviours are clearly seen in Figure 3 for those curves that have $K_{b\mathrm{P}} \gg 1$.

From $(25)_3$, it is clear that the bound drug exits the gel over the slow time scale $t = O(K_{b\mathrm{P}} L^2/D_{\mathrm{G}})$ in the limit $K_{b\mathrm{P}} \to \infty$. This simple result indicates how a system may be rationally designed to achieve slow release rate over a desired time scale. For example, if it is required that the drug slowly exits the hydrogel over a period of months, it predicts that the system should be designed with $K_{b\mathrm{P}} \gg 1$ and $K_{b\mathrm{P}} L^2/D_{\mathrm{G}} \approx 30$ days. The passive diffusion time scale is $t = O(L^2/D_{\mathrm{G}})$, so that the slow time scale is simply the diffusion time scale multiplied by the dimensionless parameter $K_{b\mathrm{P}}$. Hence, for strongly retained drugs, the effect of binding is encapsulated in the single parameter $K_{b\mathrm{P}}$.

In summary, if slow release relative to the passive diffusion time scale is required, the affinity hydrogel should be prepared with $K_{b\mathrm{P}} \gg 1$, or

$$c^{\mathrm{T0}}_{\mathrm{P}} \gg K^{\mathrm{D}}_{\mathrm{G\text{-}P}}.$$

When placed in a fluid environment, the drug then releases from the gel over the slow time scale

$$t = O(K_{b\mathrm{P}} L^2/D_{\mathrm{G}}) = O(c^{\mathrm{T0}}_{\mathrm{P}} L^2/\{K^{\mathrm{D}}_{\mathrm{G\text{-}P}} D_{\mathrm{G}}\}).$$

3.2 Numerical solutions

In this section, we display numerical solutions to the initial boundary value problem (21). The purpose here is to illustrate the wide range of release behaviours the system is capable of exhibiting, and to numerically confirm the analytical predictions of the previous section. In the numerical plots, we display the fraction of the total drug originally in the gel that has been released as a function of time. The formula for this fraction is given by (18). Many of the release behaviours exhibited here have been observed in experiments, but we postpone a comparison of theory and experiment until Section 3.3.

3.2.1 The numerical method

An explicit finite difference scheme was used to numerically integrate (21). Forward differences were used to approximate the time derivatives, centred differences for the second order spatial derivatives, and the boundary condition on $x = 0$ was handled by introducing a fictitious line in the usual way. The values for $c_{\mathrm{G}}^{\mathrm{T}}$ and $c_{\mathrm{P}}^{\mathrm{T}}$ were updated in time using (21), and the updates for the remaining quantities were then calculated using (20). The scheme was coded using the mathematical software package MATLAB.

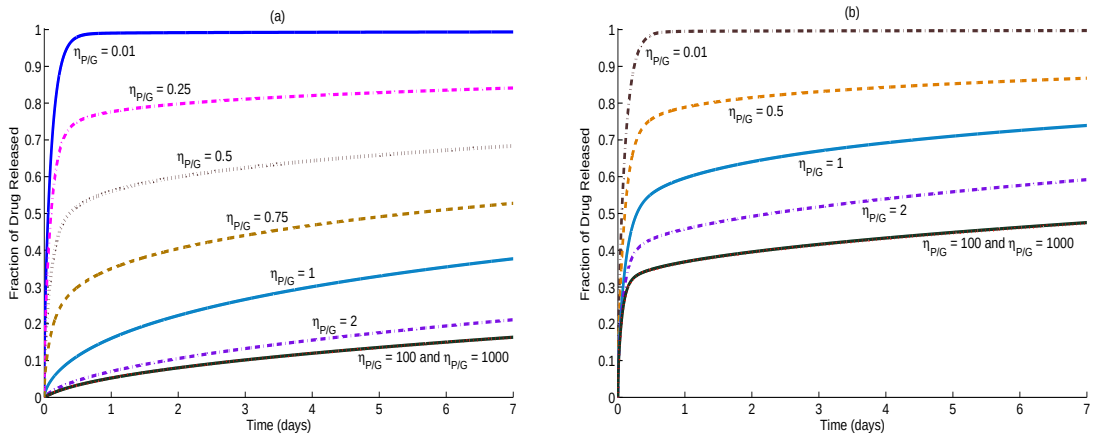

Figure 4: Numerical solutions of the initial boundary value problem (21). The predicted fraction of total drug released (see equation (18)) as a function of time over a period of a week is displayed. The parameter values chosen are $L = 0.2$ cm, $D_{\mathrm{G}} = 1 \times 10^{-4}\mathrm{cm}^2/\mathrm{min}$, $D_{\mathrm{PU}} = 1.8 \times 10^{-4}\mathrm{cm}^2/\mathrm{min}$, $D_{\mathrm{GPU}} = 9.6 \times 10^{-5}\mathrm{cm}^2/\mathrm{min}$, $K_{b\mathrm{P}} = 1000$, and various values for $\eta_{\mathrm{P/G}}$, which have been indicated on the curves. In (a), $r = 1$, so that all of the peptide is permanently fixed to the matrix. In (b), $r = 0.5$, so that half of the peptide is initially fixed to the matrix.

3.2.2 Strongly retained drug

In Figure 4, we display numerical release profiles for the case of strongly retained drug, $K_{b\mathrm{P}} \gg 1$. It is seen that the drug release rate becomes slow after a period of approximately a day. This fast initial release phase corresponds to the rapid out-diffusion of free drug and unbound drug-peptide complex on the relatively short diffusion time scale. In these calculations, $L = 0.2$ cm and $D_{\mathrm{G}} = 1 \times 10^{-4}\mathrm{cm}^2/\mathrm{min}$, so that this time scale is determined from $L^2/D_{\mathrm{G}} \approx 7$ hours, which is consistent with the displayed profiles. Once the unbound components have substantially exited the system, the remaining bound fraction releases slowly over the slow time scale determined from $K_{b\mathrm{P}}L^2/D_{\mathrm{G}}$. Figure 4 has $K_{b\mathrm{P}}L^2/D_{\mathrm{G}} \approx 1$ year.

Figure 4 (a) has $r = 1$, so that all of the peptide is permanently fixed to the matrix. Hence, provided there is sufficient peptide to bind the drug ($c_{\mathrm{P}}^{\mathrm{T0}} \geq c_{\mathrm{G}}^{\mathrm{T0}}$ or $\eta_{\mathrm{P/G}} \geq 1$), all of the drug should release slowly, and this is confirmed by inspecting the curves in Figure 4 (a) that have $\eta_{\mathrm{P/G}} \geq 1$. However, the curves in Figure 4 (a) with $\eta_{\mathrm{P/G}} < 1$ have a different character. Consider, for example, the curve that has $\eta_{\mathrm{P/G}} = 0.5$. In this case, the initial concentration of drug is twice that of the peptide. Hence, to leading order, half of the drug is initially free in the gel, and diffuses out of the system on the short diffusion time scale. This is confirmed by inspecting the $\eta_{\mathrm{P/G}} = 0.5$ curve in Figure 4 (a), where it is seen that $M(0.5\text{ days})/M(\infty) \approx 0.5$.

In Figure 4 (b), we have $r = 0.5$, so that only half of the peptide is fixed to the matrix. Hence, for $\eta_{\mathrm{P/G}} \geq 1$, we expect approximately half of the drug to be lost from the matrix on the short diffusion time scale. Inspecting the curve with $\eta_{\mathrm{P/G}} = 1$ in Figure 4 (b), it is seen that $M(0.5\text{ days})/M(\infty) \approx 0.5$. For $\eta_{\mathrm{P/G}} < 1$, larger fractions of the drug can exit the system over the diffusion time scale. Consider, for example, the curve in Figure 4 (b) that has

$\eta_{P/G} = 0.5$. In this case, approximately half of the drug is initially bound to peptide, but only half of the peptide is fixed to the matrix. Hence, only approximately one quarter of the drug is bound to the matrix initially, with the remaining three quarters free to diffuse out of the system. We do in fact see that $M(0.5 \text{ days})/M(\infty) \approx 0.75$ in the $\eta_{P/G} = 0.5$ curve of Figure 4 (b). The key features of all of the curves in Figure 4 can be understood using similar arguments.

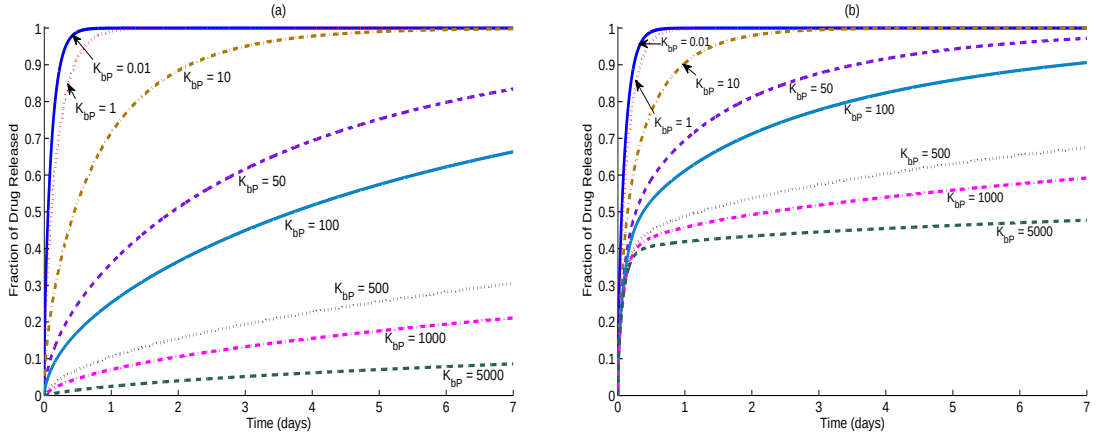

Figure 5: Numerical solutions of the initial boundary value problem (21). The predicted fraction of total drug released (see equation (18)) as a function of time over a period of a week is displayed. The parameter values chosen are $D_G = 1 \times 10^{-4}\text{cm}^2/\text{min}$, $D_{PU} = 1.8 \times 10^{-4}\text{cm}^2/\text{min}$, $D_{GPU} = 9.6 \times 10^{-5}\text{cm}^2/\text{min}$, $\eta_{P/G} = 2$, and various values for K_{bP}, which have been indicated on the curves. In (a), $r = 1$, so that all of the peptide is permanently fixed to the matrix. In (b), $r = 0.5$, so that half of the peptide is initially fixed to the matrix.

3.2.3 Varying the binding parameter K_{bP}

In Figure 5, we display numerical solutions to (21) for $\eta_{P/G} = 2$ and various values of K_{bP}, and with $r = 1$ in (a) and $r = 1/2$ in (b). The drug releases over a period of a few days for those curves that have $K_{bP} = O(1)$. The cases $K_{bP} = O(1)$ correspond to moderate retention of the drug by the hydrogel. The release rate is only slow for those curves that have $K_{bP} \gg 1$. However, there is always a fast initial release phase in the curves of Figure 5 (b) because in those cases, only half of the peptide is fixed to the matrix initially.

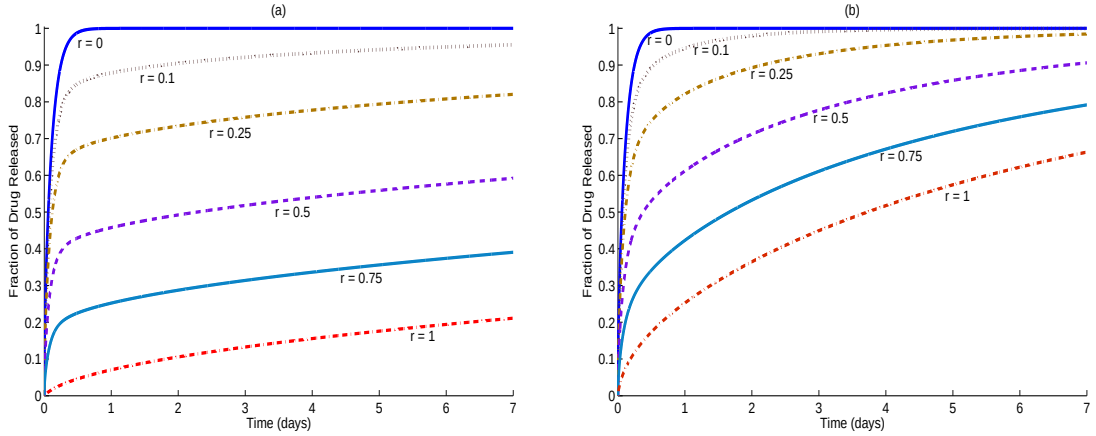

Figure 6: Numerical solutions of the initial boundary value problem (21). The predicted fraction of total drug released (see equation (18)) as a function of time over a period of a week is displayed. The parameter values used are $D_G = 1 \times 10^{-4}\text{cm}^2/\text{min}$, $D_{PU} = 1.8 \times 10^{-4}\text{cm}^2/\text{min}$, $D_{GPU} = 9.6 \times 10^{-5}\text{cm}^2/\text{min}$, $\eta_{P/G} = 2$, and various values for r, which have been indicated on the curves. In (a), $K_{bP} = 1000$, and in (b), $K_{bP} = 100$.

3.2.4 Varying the fraction of bound peptide r

In Figure 6, numerical solutions to (21) are displayed for $\eta_{\text{P/G}} = 2$ and various values of r, and with $K_{b\text{P}} = 1000$ in (a), and $K_{b\text{P}} = 100$ in (b). In Figure 6 (a), we see as expected that a fraction $(1-r)$ of the drug is lost in the first few days, but that release thereafter is slow. In Figure 6 (b), where the binding is weaker by an order of magnitude, this effect is weaker, though still discernible.

Table 2: The data used to generate the theoretical curves in Figure 7. The values for r and $K_{b\text{P}}$ were determined in this study, and the remaining parameter values were taken from Willerth *et al.* [31].

Symbol	Figure 7 (a) $K_{b\text{P}} = 110$	Figure 7 (b) $K_{b\text{P}} = 130$	Figure 7 (c) $K_{b\text{P}} = 140$	Units
D_{G}	1.01×10^{-4}	1.01×10^{-4}	1.01×10^{-4}	cm^2/min
D_{PU}	1.84×10^{-4}	1.87×10^{-4}	1.82×10^{-4}	cm^2/min
D_{GPU}	9.58×10^{-5}	9.60×10^{-5}	9.57×10^{-5}	cm^2/min
c_{P}^{T0}	2.50×10^{-4}	2.50×10^{-4}	2.50×10^{-4}	M
c_{G}^{T0}	7.57×10^{-9}	7.57×10^{-9}	7.57×10^{-9}	M
r	0.3	0.3	0.3	
pH	6.0	2.8	4.5	

3.3 Comparison with experimental data

We now compare theoretical release profiles generated by the model with in vitro experimental release data drawn from three studies. In all cases the theoretical curves were obtained by numerically solving the initial boundary value problem (21) as described above, and then using (18) to obtain the release profiles. Figure 2 gives a rough schematic of the experimental setup.

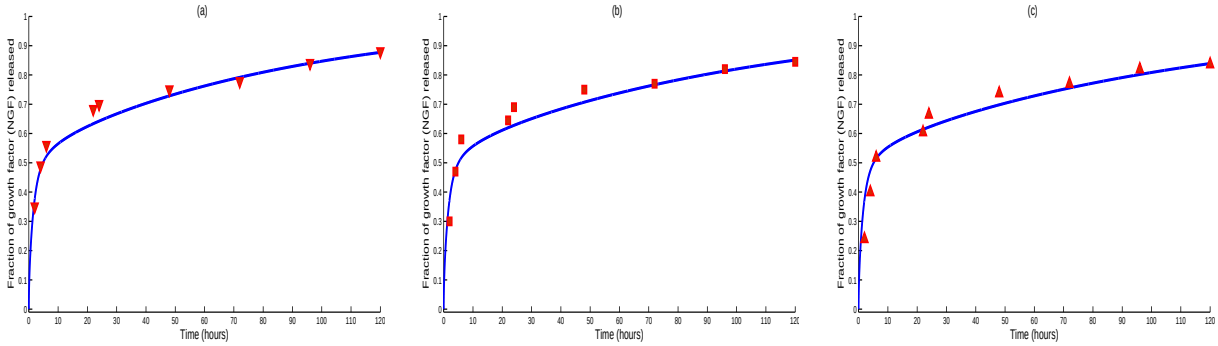

Figure 7: A comparison between the theory and experimental release profiles taken from Willerth *et al.* [31]. The curves are theoretical and the symbols are experimental. The parameter values used to generate the theoretical curves can be found in Table 2.

3.3.1 Willerth *et al.* [31]

A comparison between the theory and the experimental results of [31] is given in Figure 7. In the experiments conducted by [31], the release of the growth factor NGF from a fibrin matrix containing NGF-binding peptides was considered. The binding affinity of the peptides for the growth factor was varied by changing the pH of the elution medium. The data used to generate the theoretical curves in Figure 7 is listed in Table 2. This data was taken from [31], apart from r and $K_{b\text{P}}$ which were used as fitting parameters. The same value $r = 0.3$ was chosen for all three curves, so that 30% of the peptide was taken to be initially fixed to the fibrin matrix. However, three different values were chosen for $K_{b\text{P}}$ since the peptide affinity for the growth factor changes when the pH of the elution medium is changed. The correspondence between theory and experiment in Figure 7 is seen to be satisfactory in all cases; see Table 3 for a quantitative evaluation of the agreement between theory and experiment.

Table 3: Quantitative evaluation of the correspondence between the theoretical profiles and the experimental data points given in Figures 7 and 8. In the table, $F(t_i) = M(t_i)/M(\infty)$ is the numerical value calculated from the theoretical model at time t_i, $F_{ex}(t_i)$ is the experimental data point at time t_i, and n is the number of data points.

Figure	Mean square error $\frac{\sum_{i=1}^{n}[F(t_i)-F_{ex}(t_i)]^2}{n}$	Root mean square error $\sqrt{\frac{\sum_{i=1}^{n}[F(t_i)-F_{ex}(t_i)]^2}{n}}$
7 (a)	1.0×10^{-3}	3.2×10^{-2}
7 (b)	2.0×10^{-3}	4.5×10^{-2}
7 (c)	3.0×10^{-3}	5.5×10^{-2}
8 (a) - Weak binder	4.0×10^{-3}	6.3×10^{-2}
8 (a) - Strong binder	6.6×10^{-5}	8.1×10^{-3}
8 (b) - Weak binder	1.0×10^{-3}	3.2×10^{-2}
8 (b) - Strong binder	5.5×10^{-5}	7.4×10^{-3}

3.3.2 Pakulska *et al.* [16]

Pakulska *et al.* [16] studied the release of the bacterial enzyme ChABC from a peptide-based affinity system, and a comparison between the theory and their experimental release profiles can be found in Figure 8 (a). The parameter values used to generate the theoretical curves in Figure 8 (a) are given in its caption. These parameters were taken from [16] where available. It was necessary here to select values for the diffusivities and r as these were not available. However, the character of the theoretical release curves is not very sensitive to the values of the diffusivities, and the order of magnitude of these values is known. In Figure 8 (a), the weak binder has the value $K_{b\text{P}} \approx 17$, and the strong binder has $K_{b\text{P}} \approx 1700$. The correspondence between theory and experiment is seen to be good for the strong binder, but is less satisfactory for the weak binder (Table 3).

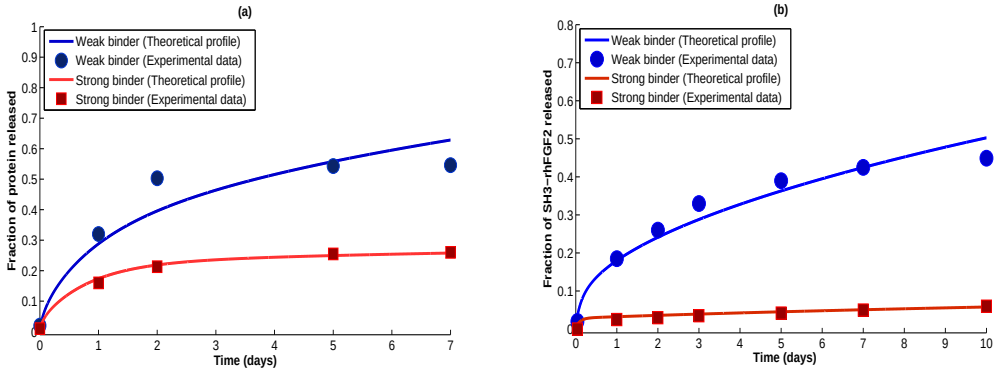

Figure 8: A comparison between the theory and experimental release profiles taken from (a) Pakulska *et al.* [16] and (b) Vulic & Shoichet [28]. In (a), the parameter values used are $c_{\text{P}}^{\text{T0}} = 4.5 \times 10^{-4}$ M, $c_{\text{G}}^{\text{T0}} = 4.5 \times 10^{-6}$ M, $r = 0.75$, $D_{\text{G}} = 1.5 \times 10^{-5}$ cm^2/min, $D_{\text{PU}} = 1.3 \times 10^{-5}$ cm^2/min and $D_{\text{GPU}} = 1.2 \times 10^{-5}$ cm^2/min. In (b), the parameter values used are $c_{\text{P}}^{\text{T0}} = 4 \times 10^{-3}$ M, $c_{\text{G}}^{\text{T0}} = 2 \times 10^{-5}$ M, $r = 0.92$, $D_{\text{G}} = 8 \times 10^{-5}$ cm^2/min, $D_{\text{PU}} = 10^{-4}$ cm^2/min and $D_{\text{GPU}} = 5 \times 10^{-5}$ cm^2/min. For the weak binder $K_{\text{G-P}}^{\text{D}} = 2.7 \times 10^{-5}$ M, and for the strong binder $K_{\text{G-P}}^{\text{D}} = 2.7 \times 10^{-7}$ M.

3.3.3 Vulic & Shoichet [28]

Vulic & Shoichet [28] used a peptide-based affinity hydrogel to control the release of recombinant human basic fibroblast growth factor (rhFGF2). Figure 8 (b) gives the comparison between the theory developed here and their release profiles. The parameter values used to generate the theoretical curves displayed are given in its caption. These values were taken from [28] where available. The correspondence between theory and experiment is again quite good here (Table 3).

4 Conclusions

Peptide-based affinity hydrogels are quite complex systems because their behaviour can depend on the binding and diffusive properties of several species. Additionally, the initial concentrations of the drug and peptide in the gel can be varied, and the choice made can significantly affect the subsequent release behaviour. Also, the initial ratio of the bound to unbound peptide in the mixture may be unknown. In view of this complexity, designing an affinity system to achieve a desired release profile is challenging. Mathematical modelling can assist with this task.

In the current study, a mathematical model for peptide-based affinity systems is formulated and analysed. For many systems, it is shown that the model may be simplified considerably. It is found that the ratio of the concentration of peptide to the dissociation constant for the drug and the peptide is frequently the key parameter in determining the release rate. Quantitative information relating the rate of release and model parameter values is presented. Output from the model is compared with the results of three different experimental release studies, and good agreement is found. Numerical solutions of the model are presented that exhibit a wide range of behaviours, underlining the considerable potential of affinity hydrogels as release systems.

Acknowledgments. We gratefully acknowledge the support of the Mathematics Applications Consortium for Science and Industry (www.macsi.ul.ie) funded by the Science Foundation Ireland (SFI) Investigator Award 12/IA/1683. Dr Meere thanks NUI Galway for the award of a travel grant. We thank the referees for their helpful suggestions to improve the paper.

References

[1] Alberts, B., A. Johnson, J. Lewis, M. Raff, K. Roberts, and P. Walter. Molecular Biology of the Cell, 5th edition. New York: Garland Science, 2008, 1392 pp.

[2] Bradbury, E. J., L. D. F. Moon, R. J. Popat, V. R. King, G. S. Bennett, P. N. Patel, J. W. Fawcett, and S. B. McMaho. Chondroitinase abc promotes functional recovery after spinal cord injury. *Nature* **416**: 636–640, 2002.

[3] Crank, J. The Mathematics of Diffusion, 2nd edition. Oxford University Press, 1975, 414 pp.

[4] Fu, A. S., T. R. Thatiparti, G. M. Saidel, and H. A. von Recum. Experimental studies and modeling of drug release from a tunable affinity-based drug delivery platform. *Annals of Biomedical Engineering* **39**: 2466–2475, 2011.

[5] Hoffman, A. S. Hydrogels for biomedical applications. *Adv. Drug Deliv. Rev.* **64**: 18–23, 2012.

[6] Hu, S. M. & S. Schmidt. Interactions in sequential diffusion processes in semiconductors. *J. Appl. Phys.* **39**: 4272, 1968.

[7] Hubbell, J. A. Matrix-bound growth factors in tissue repair. *Swiss. Med. Wkly* **136**: 387–391, 2006.

[8] King, J. R. & C. P. Please. Diffusion of dopant in crystalline silicon: an asymptotic analysis. *IMA J. Appl. Math.* **37**: 185–197, 1986.

[9] Lin, C. C. and K. S. Anseth. Controlling affinity binding with peptide-functionalized poly(ethylene glycol) hydrogels. *Adv. Funct. Mater.* **19**: 2325–2331, 2009.

[10] Lin, C. C., A. T. Metters, and K. S. Anseth. Functional peg-peptide hydrogels to modulate local inflammation induced by the pro-inflammatory cytokine tnfα. *Biomaterials* **30**: 4907–4914, 2009.

[11] Lin, C. C., and A. T. Metters. Metal-chelating affinity hydrogels for sustained protein release. *Journal of Biomedical Materials Research Part A* **83A**: 954964, 2007.

[12] Lin, C. C., P. D. Boyer, A. A Aimetti, and K. S. Anseth. Regulating mcp-1 diffusion in affinity hydrogels for enhancing immuno-isolation. *J. Control. Release* **142**: 384–391, 2010.

[13] Maxwell, D. J., B. C. Hicks, S. Parsons, and S. E. Sakiyama-Elbert, Development of rationally designed affinity-based drug delivery systems. *Acta Biomater.* **1**: 101–113, 2005.

[14] Maynard, H. D. and J. A. Hubbell. Discovery of a sulfated tetrapeptide that binds to vascular endothelial growth factor. *Acta Biomater.* **1**: 451–459, 2005.

[15] Mohtaram, N. K., A. Montgomery, and S. M. Willerth. Biomaterial-based drug delivery systems for the controlled release of neurotrophic factors. *Biomed. Mater.* **8**: 022001 (1–13), 2013.

[16] Pakulska, M. M, K. Vulic, and M. S. Shoichet. Affinity-based release of chondroitinase abc from a modified methylcellulose hydrogel. *J. Control. Release* **171**: 11–16, 2013.

[17] Please, C. P. & J. R. King. One- and two-dimensional nonlinear dopant diffusion in crystalline silicon - some analytical results. *Solid State Electronics.* **31**: 299-305, 1988.

[18] Sakiyama-Elbert, S. E. and J. A. Hubbell, Development of fibrin derivatives for controlled release of heparin-binding growth factors. *J. Control. Release* **65**: 389–402, 2000.

[19] Shepard, J. A., P. J. Wesson, C. E. Wang, A. C. Stevans, S. J. Holland, A. Shikanov, B. A. Grzybowski, and L. D. Shea. Gene therapy vectors with enhanced transfection based on hydrogels modified with affinity peptides. *Biomaterials* **32**: 5092–5099, 2011.

[20] Siepmann, J. and F. Siepmann. Mathematical modelling of drug delivery. *Int. J. Pharm.* **364**: 328–343, 2008.

[21] Tzafriri, A. R., A. D. Levin, and E. R. Edelman. Diffusion-limited binding explains binary dose response for local arterial and tumour drug delivery. *Cell Proliferation* **42**: 348–363, 2009.

[22] Varki, A., R. D. Cummings, J. D. Esko, H. H. Freeze, P. Stanley, C. R. Bertozzi, G. W. Hart, and M. E. Etzler. Essentials of glycobiology, 2nd edition. New York: Cold Spring Harbor Laboratory Press, 2009, 784pp.

[23] Vo, T. T. N., R. Yang, Y. Rochev, and M. G. Meere. A mathematical model for drug delivery. *Progress in IndustrialMathematics at ECMI 2010*: 521–528, 2010.

[24] Vo, T. T. N. and M. G. Meere. Minimizing the passive release of heparin-binding growth factors from an affinity-based delivery system. *Mathematical Medicine and Biology* **29**: 1–26, 2012.

[25] Vo, T. T. N. and M. G. Meere. The mathematical modelling of affinity-based drug delivery systems. Submitted to the *Journal of Coupled Systems and Multiscale Dynamics.*

[26] Vo, T. T. N. Mathematical analysis of some models for drug delivery, PhD thesis. Galway: National University of Ireland Galway, 2012.

[27] Vulic, K., M. M. Pakulska, R. Sonthalia, A. Ramachandran, and M. S. Shoichet. Mathematical model accurately predicts protein release from an affinity-based delivery system. *Journal of Controlled Release.* **197**: 69-77, 2015.

[28] Vulic, K. and M. S. Shoichet. Tunable growth factor delivery from injectable hydrogels for tissue engineering. *J. Am. Chem. Soc.* **134**: 882–885, 2012.

[29] Vulic, K. and M. S. Shoichet. Affinity-based drug delivery systems for tissue repair and regeneration. *Biomacromolecules.* **15**: 3867–3880, 2014.

[30] Wang, N. X. and H. A. von Recum. Affinity-based drug delivery. *Macromol. Biosci.* **11**: 321–332, 2011.

[31] Willerth, S. M., P. J. Johnson, D. J. Maxwell, S. R. Parsons, M. E. Doukas, and S. E. Sakiyama-Elbert. Rationally designed peptides for controlled release of nerve growth factor from fibrin matrices. *J. Biomed. Mater. Res. Part A* **80A**: 13–23, 2007.

[32] Wood, M. D., A. M. Moore, D. A. Hunter, S. Tuffaha, G. H. Borschel, S. E. Mackinnon, and S. E. Sakiyama-Elbert. Affinity-based release of glial-derived neurotrophic factor from fibrin matrices enhances sciatic nerve regeneration. *Acta Biomater.* **5**: 959–968, 2009.

[33] Wood, M. D. and S. E. Sakiyama-Elbert. Release rate controls biological activity of nerve growth factor released from fibrin matrices containing affinity-based delivery systems. *J. Biomed. Mater. Res. Part A* **84A**: 300–312, 2008.

Appendix

In this appendix, we outline the asymptotic analysis of the initial boundary value problem (23) for the limit $K_{b\mathrm{P}} \to \infty$. We begin by displaying the non-dimensional form for the equations. We recall that the non-dimensional variables are

$$\bar{x} = \frac{x}{L}, \quad \bar{t} = \frac{t}{(L^2/D_{\mathrm{G}})}, \quad \bar{c}_{\mathrm{G}}^{\mathrm{T}} = \frac{c_{\mathrm{G}}^{\mathrm{T}}}{c_{\mathrm{G}}^{\mathrm{T0}}}, \quad \text{and} \quad \eta_{\mathrm{P/G}} = \frac{c_{\mathrm{P}}^{\mathrm{T0}}}{c_{\mathrm{G}}^{\mathrm{T0}}}$$

and these lead to the following non-dimensional form (dropping the over-bars)

$$\begin{aligned}
&\frac{\partial c_{\mathrm{G}}^{\mathrm{T}}}{\partial t} = \frac{\partial}{\partial x}\left(D_{\mathrm{GG}}^{\mathrm{T}}(c_{\mathrm{G}}^{\mathrm{T}}) \frac{\partial c_{\mathrm{G}}^{\mathrm{T}}}{\partial x} \right), \\
&\frac{\partial c_{\mathrm{G}}^{\mathrm{T}}}{\partial x}(0,t) = 0 \quad \text{for } t \geq 0, \\
&c_{\mathrm{G}}^{\mathrm{T}}(1,t) = 0 \quad \text{for } t \geq 0, \\
&c_{\mathrm{G}}^{\mathrm{T}}(x,0) = 1 \quad \text{for } 0 < x < 1,
\end{aligned} \tag{26}$$

where

$$D_{\mathrm{GG}}^{\mathrm{T}}(c_{\mathrm{G}}^{\mathrm{T}}) = \frac{1}{2}\left(1 + \frac{K_{b\mathrm{P}}\,(c_{\mathrm{G}}^{\mathrm{T}} - \eta_{\mathrm{P/G}}) + \eta_{\mathrm{P/G}}}{\sqrt{\left[K_{b\mathrm{P}}\,(c_{\mathrm{G}}^{\mathrm{T}} - \eta_{\mathrm{P/G}}) - \eta_{\mathrm{P/G}}\right]^2 + 4K_{b\mathrm{P}}\eta_{\mathrm{P/G}}c_{\mathrm{G}}^{\mathrm{T}}}} \right). \tag{27}$$

We shall discuss the case $\eta_{\mathrm{P/G}} < 1$, which corresponds to there being a higher concentration of drug than peptide in the gel initially. In the limit $K_{b\mathrm{P}} \to \infty$, there are three time scales to consider, two of which we shall discuss.

4.1 Short time scale $t = O(1)$

In dimensional terms this corresponds to $t = O(L^2/D_{\mathrm{G}})$, the diffusion time scale. This is the time scale over which the unbound drug fraction substantially out-diffuses from the gel. The asymptotic structure for $t = O(1)$ as $K_{b\mathrm{P}} \to \infty$ is depicted schematically in Figure S1 in the Supplementary Material. It may be helpful to refer to this figure in the coming analysis.

In $t = O(1)$, $x = O(1)$, we pose $c_{\mathrm{G}}^{\mathrm{T}} \sim c_{\mathrm{T0}}^{s}(x,t)$ as $K_{b\mathrm{P}} \to \infty$, to obtain the linear problem

$$\begin{aligned}
&\frac{\partial c_{\mathrm{T0}}^{s}}{\partial t} = \frac{\partial^2 c_{\mathrm{T0}}^{s}}{\partial x^2}, \\
&\frac{\partial c_{\mathrm{T0}}^{s}}{\partial x}(0,t) = 0 \quad \text{for } t \geq 0, \\
&c_{\mathrm{T0}}^{s}(1,t) = \eta_{\mathrm{P/G}} \quad \text{for } t \geq 0, \\
&c_{\mathrm{T0}}^{s}(x,0) = 1 \quad \text{for } 0 < x < 1.
\end{aligned} \tag{28}$$

This linear problem can be solved using the method of separation of variables [3], to obtain

$$c_{\mathrm{T0}}^{s}(x,t) = \eta_{\mathrm{P/G}} + \frac{4(1-\eta_{\mathrm{P/G}})}{\pi} \sum_{n=1}^{\infty} \frac{(-1)^{n+1}}{2n-1} \exp\left(\frac{-(2n-1)^2\pi^2 t}{4} \right) \cos\left(\frac{(2n-1)\pi x}{2} \right). \tag{29}$$

The perfect sink boundary conditions in (26) are not met by this solution since $c_{\mathrm{T0}}^{s}(1,t) = \eta_{\mathrm{P/G}}$. The solution drops from approximately $\eta_{\mathrm{P/G}}$ to small values over two asymptotically narrow regions near the interface $x = 1$, and we now discuss these.

$x^*, t = O(1),\ x = 1 + K_{b\mathrm{P}}^{-1/2} x^*$

Writing $c_{\mathrm{G}}^{\mathrm{T}}(x,t) = \eta_{\mathrm{P/G}} + K_{b\mathrm{P}}^{-1/2} c_{\mathrm{T}}^{*}(x^*,t)$ and posing $c_{\mathrm{T}}^{*} \sim c_{\mathrm{T0}}^{*}(x^*,t)$ in $x^*, t = O(1)$ as $K_{b\mathrm{P}} \to \infty$, one obtains

$$\frac{\partial}{\partial x^*}\left(D_{\mathrm{eff}}(c_{\mathrm{T0}}^{*}) \frac{\partial c_{\mathrm{T0}}^{*}}{\partial x^*} \right) = 0,$$

where

$$D_{\mathrm{eff}}(c_{\mathrm{T0}}^{*}) = \frac{1}{2}\left(1 + \frac{c_{\mathrm{T0}}^{*}}{\sqrt{{c_{\mathrm{T0}}^{*}}^2 + 4{\eta_{\mathrm{P/G}}}^2}} \right).$$

Integrating this equation twice gives

$$c_{\mathrm{T0}}^{*} = \frac{(\gamma(t)x^* + \nu(t))^2 - 4\eta_{\mathrm{P/G}}^2}{2\,(\gamma(t)x^* + \nu(t))},$$

where $\gamma(t), \nu(t)$ are determined by matching. Imposing $|c^*_{\mathrm{T0}}| \to \infty$ as $x^* \to 0^-$ implies that $\nu(t) = 0$, and then

$$c^*_{\mathrm{T0}} = \frac{\gamma(t)^2 x^{*2} - 4\eta^2_{\mathrm{P/G}}}{2\gamma(t)x^*}. \tag{30}$$

The function $\gamma(t)$ is determined by matching the drug fluxes in $x = O(1)$ and $x^* = O(1)$; we have that

$$\lim_{x\to 1^-}\left(-\frac{\partial c^s_{\mathrm{T0}}}{\partial x}\right) = \lim_{x^*\to-\infty}\left(-D^s_{\mathrm{eff}}(c^*_{\mathrm{T0}})\frac{\partial c^*_{\mathrm{T0}}}{\partial x^*}\right),$$

which immediately yields that

$$\gamma(t) = 4(\eta_{\mathrm{P/G}} - 1)\sum_{n=1}^{\infty}\exp\left(\frac{-(2n-1)^2\pi^2 t}{4}\right).$$

In view of the behavior of (30) as $x^* \to 0^-$, it is clear that another scaling is required, and we now discuss this.

$\hat{x}, t = O(1),\ x = 1 + K_{b\mathrm{P}}^{-1}\hat{x}$

In $\hat{x}, t = O(1)$, we pose $c^{\mathrm{T}}_{\mathrm{G}} \sim \hat{c}_{\mathrm{T0}}(\hat{x}, t)$ as $K_{b\mathrm{P}} \to \infty$, to obtain

$$\frac{\partial}{\partial \hat{x}}\left(\frac{\eta^2_{\mathrm{P/G}}}{(\eta_{\mathrm{P/G}} - \hat{c}_{\mathrm{T0}})^2}\frac{\partial \hat{c}_{\mathrm{T0}}}{\partial \hat{x}}\right) = 0.$$

Integrating this expression twice and imposing $\hat{c}_{\mathrm{T0}} \to 0$ as $\hat{x} \to 0^+$ gives

$$\hat{c}_{\mathrm{T0}} = \frac{\eta_{\mathrm{P/G}}\delta(t)\hat{x}}{\delta(t)\hat{x} + \eta_{\mathrm{P/G}}},$$

where the function $\delta(t)$ is now determined by matching drug fluxes in $x^* = O(1)$ and $\hat{x} = O(1)$. It is found that

$$\lim_{\hat{x}\to-\infty}\left(\frac{\eta^2_{\mathrm{P/G}}}{(\eta_{\mathrm{P/G}} - \hat{c}_{\mathrm{T0}})^2}\frac{\partial \hat{c}_{\mathrm{T0}}}{\partial \hat{x}}\right) = \lim_{x^*\to 0^-}\left(D_{\mathrm{eff}}(c^*_{\mathrm{T0}})\frac{\partial c^*_{\mathrm{T0}}}{\partial x^*}\right) = \gamma(t),$$

which gives

$$\delta(t) = \gamma(t),$$

completing the asymptotic analysis for $t = O(1)$.

4.2 Long time scale $t = O(K_{b\mathrm{P}})$

In dimensional terms, this corresponds to $t = O(K_{b\mathrm{P}}L^2/D_{\mathrm{G}})$. This is the time scale over which the drug substantially exits the gel, and so is of importance from the point of view of applications.

Writing $t = K_{b\mathrm{P}}T$, we pose $c^{\mathrm{T}}_{\mathrm{G}} \sim c^{\mathrm{L}}_{\mathrm{T0}}(x, T)$ in $T = O(1)$, $0 < x < 1$ as $K_{b\mathrm{P}} \to \infty$ to obtain the leading order problem

$$\begin{aligned}
&\frac{\partial c^{\mathrm{L}}_{\mathrm{T0}}}{\partial T} = \frac{\partial}{\partial x}\left(\frac{\eta^2_{\mathrm{P/G}}}{(\eta_{\mathrm{P/G}} - c^{\mathrm{L}}_{\mathrm{T0}})^2}\frac{\partial c^{\mathrm{L}}_{\mathrm{T0}}}{\partial x}\right),\ 0 < x < 1, T > 0,\\
&\frac{\partial c^{\mathrm{L}}_{\mathrm{T0}}}{\partial x}(0, T) = 0,\ c^{\mathrm{L}}_{\mathrm{T0}}(1, T) = 0 \quad \text{for } T \geq 0,\\
&c^{\mathrm{L}}_{\mathrm{T0}}(x, T) \to \eta_{\mathrm{P/G}} \quad \text{as } T \to 0,\ 0 < x < 1.
\end{aligned} \tag{31}$$

Here $c^{\mathrm{L}}_{\mathrm{T0}} \to 0$ as $T \to \infty$, and so the drug is eliminated from the matrix on this time scale.

There is another time scale intermediate to $t = O(1)$ and $t = O(K_{b\mathrm{P}})$, but this case is of limited practical interest and is not discussed here.